Aquaculture Reports 19 (2021) 100582

Contents lists available at ScienceDirect

Aquaculture Reports

journal homepage: www.elsevier.com/locate/aqrep

Genome-wide identification and expression profiling revealed tissue-specific inducible expression of cytochrome P450s conferring cadmium tolerance in the Pacific oyster, *Crassostrea gigas*

Jing Tian [a], Zexin Jiao [a], Huiru Fu [a], Lu Qi [a], Qi Li [a,b], Nannan Liu [c], Shikai Liu [a,b,*]

[a] Key Laboratory of Mariculture (Ocean University of China), Ministry of Education, and College of Fisheries, Ocean University of China, Qingdao, 266003, China
[b] Laboratory for Marine Fisheries Science and Food Production Processes, Qingdao National Laboratory for Marine Science and Technology, Qingdao, 266237, China
[c] Department of Entomology and Plant Pathology, Auburn University, Auburn, AL 36849, USA

ARTICLE INFO

Keywords:
Cytochrome P450
Pacific oyster
Cadmium
Sequence analyses
Expression

ABSTRACT

Cytochrome P450s (CYPs) are present in almost all organisms and play critical roles in metabolism of endogenous substrates and detoxification of xenobiotic compounds. Oysters are a group of bivalves that are important in marine ecosystem and aquaculture program, adapting to the harsh environment in intertidal zones. The studies on CYPs and their potential involvement in dealing with toxic xenobiotics in oysters were limited. In the present study, we performed a multiple omics analyses and identified a full-set of 123 CYP genes in the Pacific oyster, *Crassostrea gigas*. These CYP genes were classified into 5 clans and 16 families. The phylogenetic tree constructed with other species showed extensive gene expansion of CYPs in the clan 2 and mitochondrial clan in the *C. gigas*. The amino acid sequence analysis showed conserved typical motifs of CYP genes. The expression profiles of CYPs quantified across different tissues (gill and digestive gland) at various time points (0d, 0.5d, 7d, 14d, 28d) revealed their roles in response to Cd exposure. Notably, CYP17A1-like_6 and CYP2C50 were expressed at significantly higher levels compared with other CYP genes, suggesting their crucial roles in the detoxification of Cd in the *C. gigas*. This work provides valuable information toward understanding of CYP-mediated detoxification of cadmium in mollusks, and will be important for surveillance of marine environment pollution and seafood safety.

1. Introduction

Cytochrome P450s (CYPs), named for their characteristic spectral property of Soret absorption peak at 450 nm when binding with carbon monoxide, constitute a widespread and highly diverse heme-thiolate enzyme superfamily (Werck-Reichhart and Feyereisen, 2000; Zhang et al., 2014). To date, CYPs are well known to play critical roles in catalyzing phase I oxidative, reductive and peroxidative reactions of both endogenous substances and xenobiotics to detoxified forms, or in some cases, harmful reactive intermediates (Tian et al., 2014). Particularly, CYPs in families 1–4 are important to the phase I detoxification systems of vertebrates, invertebrates, and plants (Baldwin et al., 2009). Furthermore, CYPs are involved in providing tolerance or resistance to environmental chemicals in diverse organisms. For instance, pesticide resistance in insects is associated with the number of CYP genes (Liu et al., 2015). In oysters, the hyper-accumulation of metals has been documented for several metals, especially Cu, Zn, and Cd (Wang et al., 2018). The activity of cytochrome P450-dependent system is inducible after exposure to organic xenobiotics, which are subsequently metabolized (Meng et al., 2018; Porte et al., 2001). All these CYPs are classified into clans, families and subfamilies based on sequence similarities, phylogenetic and syntenic relationships (Nebert et al., 1987; Nelson et al., 2004). At present, thousands of CYPs have been identified from virus to humans, and vast information has been uploaded into the CYP database (http://drnelson.uthsc.edu/CytochromeP450.html). However, relatively fewer CYP gene families have been determined in marine mollusks compared to vertebrates and terrestrial invertebrates. Only a few species, including *Chlamys farreri*, *Ruditapes philippine, Mactra chinensis*, *Mytilus edulis*, *Mytilus coruscus*, *Crassostrea brasiliana* have identified partial CYP families, e.g., CYP1-like, CYP2, CYP3-like, CYP4 and

* Corresponding author at: Key Laboratory of Mariculture (Ocean University of China), Ministry of Education, and College of Fisheries, Ocean University of China, China.
E-mail address: liushk@ouc.edu.cn (S. Liu).

https://doi.org/10.1016/j.aqrep.2020.100582
Received 20 August 2020; Received in revised form 18 December 2020; Accepted 20 December 2020
Available online 4 January 2021

CYP356 (Pan et al., 2011; Tian et al., 2014; Toledo-Silva et al., 2008; Zanette et al., 2013; Zhang et al., 2010, 2019; Zhang et al., 2016).

Oysters are worldwide distributed mollusks, known to bio-accumulate and tolerate high concentrations of heavy metals. The concentration of accumulated heavy metals in their soft tissues can be up to 10^4 times higher than those in seawater (Poteat et al., 2013). Therefore, they are extensively used as bio-monitors for metal pollution and eco-toxicological studies (Alfonso et al., 2013; Funes et al., 2006; O'Connor, 2002). Heavy metals are serious pollutants due to their persistence and bioaccumulation into the food chains. Among toxic metal pollutants, cadmium (Cd) is one of the most harmful metals, and is detrimental to humans, marine organisms and ecosystems (Huang et al., 2019; Sun et al., 2018). Oysters are not only the key species in estuarine environments but also one of the major seafood for human consumption. The level of accumulated Cd is highly related to seafood safety, therefore it is crucial to determine Cd level and understand molecular mechanism for bioaccumulation.

The CYP450 is reported to be a key enzyme in many detoxification pathways, and its role in metal detoxification has been reported in some species (Liu et al., 2019; Zhang et al., 2019). In vertebrates, heavy metals have been reported to affect CYP expression or activity in mice, chickens, zebrafish and many others (Abu-Bakar et al., 2004; Chen and Chan, 2018; Cong et al., 2019; Yue et al., 2018). In bivalves, some studies reported that the transcription level of a few CYP3A family genes were significantly induced when mussels, scallops and oysters were exposed to heavy metals or aromatic hydrocarbons, suggesting a potential role in metabolic clearance in xenobiotics (Tian et al., 2014; Zanette et al., 2013). Meng et al. (2017) demonstrated that the protein abundance of one CYP increased after Cd exposure, indicating its important role in Cd defense. Besides, CYP1A1 can be up-regulated under mercury and aromatic compounds exposures (Boutet et al., 2004; Chen and Chan, 2018; Korashy and El-Kadi, 2004; Larigot et al., 2018). Although CYP may play an important role in detoxification of shellfish, there have been few studies investigated on the CYP family in oysters. Zanette et al. (2010) identified a total 39 CYP genes based on the EST database in the *C. gigas*. Sequencing of the oyster genome revealed that CYP genes were significantly expanded in the *C. gigas* (Zhang et al., 2012). Therefore, systematic identification and expression profiling of CYP genes in the *C. gigas* may contribute to understand the diversity of CYPs and reveal the CYP function in marine invertebrate class.

In this study, we conducted a systematic identification of 123 CYP genes from the Pacific oyster genome, and determined their identities based on phylogenetic relationships. According to the available transcriptome data, we analyzed the expression profiles of these CYPs after Cd exposure. Furthermore, the expression pattern of 14 CYP genes in response to Cd exposure were validated. This allowed us to identify CYP17A1-like_6 and CYP2C50 as two candidate CYPs that may play critical roles in Cd detoxification. This work provides a basis for further investigations on the biological function of CYPs in the *C. gigas*, particularly concerning the potential role of CYPs in the metabolism of heavy metals.

2. Materials and methods

2.1. Identification and nomenclature of CYP genes in the C. gigas

To identify CYP genes in the *C. gigas*, the available CYP sequences from representative invertebrates (*Crassostrea virginica*, *Caenorhabditis elegans*, *Drosophila melanogaster*, *Strongylocentrotus purpuratus*, *Exaiptasia pallida*) and vertebrates (*Homo sapiens*, *Mus musculus*, *Danio rerio*, *Gallus gallus*, *Xenopus laevis*) were used as queries. The CYP protein sequences of reference species were downloaded from the Ensembl (http://www.ensembl.org) and NCBI (http://www.ncbi.nlm.nih.gov/) databases. The BLAST searches were performed to obtain the initial pool of CYP gene sequences with a cutoff ; E-value of 1e-10. A unique set of sequences were retained after removing the repeated entries for further analysis. The identified sequences were named based on the homology of *C. gigas* CYP to those of other species using the standardized nomenclature previously assigned by Nelson et al. (2004). The root symbol CYP is followed by a number for families (generally groups of proteins with more than 40 % amino-acid sequence identity, of which there are over 200), a letter for subfamilies (greater than 55 % identity) and a number for the gene (Werck-Reichhart and Feyereisen, 2000). There are also designations for clades of CYP families (clans are named from the lowest family number in the clade, which can be defined as groups of genes that clearly diverged from a single common ancestor) (Nelson, 1999).

2.2. Phylogenetic analyses of the CYP gene family

To examine the divergence of encoding CYP genes, all deduced CYP genes and those retrieved from several representative species were used to perform the phylogenetic analysis. The full-length amino acid sequences of CYP from humans (*Homo sapiens*), zebrafish (*Danio rerio*), chicken (*Gallus gallus*), American oysters (*Crassostrea viriginica*), *Caenorhabditis elegans*, *Drosophila melanogaster*, were also included for phylogenetic analysis. Protein sequences were aligned by MAFFT followed by removal of poorly aligned amino acid positions using Gblocks (Castresana, 2000; Katoh et al., 2002). Phylogenetic analyses were carried out using the maximum likelihood (ML) method. ML analyses were performed with IQ-TREE (Nguyen et al., 2015) using the optimization model, with 1000 ultrafast bootstraps. Branches were considered to be strongly supported if bootstrap values were >70 % (Hillis and Bull, 1993; Wilcox et al., 2002). Finally, the PHY.contree output format was used to visualize the phylogenetic tree with Interactive Tree of Life (iTOL, http://itol.embl.de/).

2.3. Sequence analyses of CYPs in the C. gigas

According to the deduced amino acid composition, protein characteristics were predicted by the ProtParam tool (Gawenis et al., 2002), (http://www.expasy.ch/tools/protparam.html). Conserved CYP enzyme domain was predicted through the conserved domain database (CDD, https://www.ncbi.nlm.nih.gov/Structure/cdd/wrpsb.cgi) at the NCBI server. The conserved motifs of CYP proteins were observed with MEME software (Brown et al., 2013), (http://meme-suite.org/tools/meme). The optimum widths of motifs were set as 6–50 amino acids, the maximum number of motifs was selected as 8 and the other parameters were set by default.

2.4. Cadmium exposure experiment and sample collection

Ten-month-old Pacific oysters (average 57.78 ± 0.56 mm in shell height, 25.44 ± 0.32 mm in shell length, 14.56 ± 0.19 mm in shell width, 12.71 ± 0.25 g in body weight) were taken from an oyster farm in Weihai, China, in April 2019, and acclimated for one week before experiment. After acclimation, a total of 210 oysters were divided into six tanks with 30 L filtered seawater for Cd exposure experiment. Oysters in three tanks were exposed to seawater with 200 μg/L Cd using as treatment groups, and the other three were exposed to seawater without Cd using as control groups. The Cd exposure concentration was determined based on previous studies which was below lethal level but sufficient to alter the antioxidant system of shellfish (Pan, 2015). During experiment, the oysters were maintained in filtered seawater (pH 8.03 ± 0.1, salinity 30 ± 1) at 17 ± 1 °C. The seawater was changed every day for each tank and the oysters were fed with concentrated *Chlorella vulgaris* fluid (4.3×10^5 cells/mL) every other day to minimize metal transfer via the trophic exposure route. Before the water is exchanged, the cadmium-containing tank is added three times the concentration of sodium sulfide for half an hour before the water is discharged to avoid pollution to the environment.

For sample collection, three oysters were collected from each tank

for each time point (12h, 7d, 14d, 28d). Gill and digestive gland were sampled as these two tissues form an active site for xenobiotic uptake and oxy-radical generation as well as enzyme biotransformation process (Livingstone et al., 1992). The same tissue of the three oysters in each tank at the same time point were pooled as a mixed sample, leading to three replicates per treatment at each time point. The collected tissues were immediately frozen in liquid nitrogen and stored at −80 °C freezer for use. All tissues of each treatment from three tanks were homogenized and used for measurement of cadmium content.

2.5. Measurement of cadmium content in gill and digestive gland

The tissues in each treatment group were ground to powder using agate mortar, pestle and liquid nitrogen. About 0.5 g homogenate of different tissues were thoroughly digested in concentrated HNO_3 and H_2O_2. This mixture was boiled, and Cd contents were determined by inductively coupled plasma-atomic emission spectroscopy (ICP-AES) using an Agilent 720-ES (Agilent Technologies, USA) after cooling. The detection limit for Cd was ~0.02 ppm (mg/L). The operating conditions of ICP-AES (Agilent 720-ES) were set as follows: RF Power was 1.20KW; Plasma flow was 15.0 L/min; Auxiliary flow was 1.50 L/min; Nebulizer flow was 0.75 L/min; Sample uptake delay was 15 s; Instr stabilization delay was 15 s; Replicate read time was 2 s; Replicates were 3 times.

2.6. RNA extraction and quantitative real-time PCR validation

RNA was extracted from the gill and digestive gland for Cd treatment group and control group, respectively. Total RNA of each sample was extracted with TRIzol reagent (Invitrogen, USA) following the manufacturer's instructions. The RNA quality was measured via Nanodrop2000 (Thermo Scientific) at A260 and A280. The RNA integrity was assessed via electrophoresis in a 1.2 % agarose gel.

Six RNA-Seq data sets (SRA accession numbers SRR334313, SRR334300, SRR334310, SRR334312, SRR334295 and SRR334308) were used in this study to identify potential key CYP genes that play critical roles in the *C. gigas* upon cadmium exposure. The RNA-seq analysis was conducted following the HISAT-StringTie-Ballgown protocol (Pertea et al., 2016). Briefly, raw RNA sequencing reads in fastq format were trimmed using Fastp program to obtain clean reads for subsequent analysis. The reference oyster genome (oyster_v9, NCBI accession: GCF_000297895.1) was indexed using HISAT2 (Kim et al., 2015), followed by read mapping of the clean reads. After obtaining the sorted bam files, StringTie (Pertea et al., 2015) was used to assemble transcripts and then merge transcripts from all samples. StringTie was also used for estimating transcript abundances and create table counts. Transcript expression was calculated using the FPKM method (expected number of Fragments Per Kilobase of transcript sequence per Millions of base pairs sequenced), which simultaneously considers the effect of sequencing depth and gene length for the read counts (Garber et al., 2011). The differential expression analysis between two groups was performed using the R package DESeq (1.18.0) (Anders and Huber, 2010). Genes with fold-change cutoff of 2 and P-value < 0.05 were identified as differentially expressed genes. This allowed us to identify 14 differentially expressed CYP genes for further qRT-PCR analysis.

For qRT-PCR analysis, 5 μL RNA (200 ng/μL) was reversely transcribed using the PrimeScript™RT reagent Kit with gDNA Eraser (Perfect Real Time) (Takara, RR047A), and qRT-PCR was performed using a LightCycler480 II Real-Time Detection System (Roche). The primers used for qRT-PCR are shown in Table 1. The amplification efficiency of the primers was tested by running a serial cDNA dilution calibration curve, and the melting curves were performed to ensure the specificity of amplification products. The elongation factor gene (EF) was chosen as the internal standard. The qRT-PCR analysis was carried out in triplicate in a total volume of 10 μL containing 5 μL of SYBR Green PCR Master Mix (QIAGEN), 2 μL of 1:10 diluted cDNA, 0.7 μL each of the forward and reverse primers (10 μM) and 1.6 μL of RNase-free water. The PCR program involved two steps: 95 °C for 2 min, followed by 40 cycles at 95 °C for 5 s and 60 °C for 10 s. The relative expression levels in each gene were calculated according to the comparative $2^{-\Delta\Delta Ct}$ method.

Table 1
Primers used for real-time quantitative PCR assay.

Gene ID	Primer	Nucleotide Sequence (5′-3′)
LOC105349146	CYP1A1_2-Forward	GGTAGATTGACCATCCCTGAGC
	CYP1A1_2-Reverse	TTGAAAGGTTTGGGCTGGAT
LOC105320754	CYP1A1_4-Forward	GCCACCATTCTTCTCCATCA
	CYP1A14-Reverse	ACCTCAAGCATTCCAGCATT
LOC105333812	CYP2C50-Forward	TTCCAGAGCCTACCAAATTCCAAC
	CYP2C50-Reverse	GCGAGCGAATCTCCTAAGCAC
LOC105327174	CYP4F22_1-Forward	ATGCCGACACAGGTAAAAGC
	CYP4F22_1-Reverse	TACAACCAGGGCGACTTATTT
LOC105329926	CYP2B19_1-Forward	ATCGGAACTGCGGAAGGTG
	CYP2B19_1-Reverse	TTTCATTGTGTCTTCCTCCAG
LOC105326181	CYP49a1_2-Forward	TTCCAGGTAGAAATCAAGAATGCG
	CYP49a1_2-Reverse	TGCGATGAACAGGTCAAGAAGG
LOC105340978	CYP2B4−3-Forward	AAGACGATTGTTGTTGTCAGTGG
	CYP2B4−3-Reverse	CTCAGAGCGTTCAGGGTAAAA
LOC105346613	CYP24-Forward	CTCATCCCAGAGGTTCCAGTT
	CYP24-Reverse	CCGTCTTCTCCGATTCTATCACTA
LOC105323364	CYP4V2-Forward	TACAGAGGGAAAGGTCAAAGGTT
	CYP4V2-Reverse	CATCTGGGTTAGCACCAATCA
LOC105348415	CYP17A1-like_3-Forward	GGACGAAATGCTCACAGTTCTTAG
	CYP17A1-like_3-Reverse	GAACGAGGTGCGTATCATCCA
LOC105327173	CYP4F22_2-Forward	CGGACAGTGCTTGCTACATTG
	CYP4F22_2-Reverse	GACACCTATCGTGGGGCGG
LOC105340526	CYP27C1-Forward	ATCCAGAAATCCAGCAGAGG
	CYP27C1-Reverse	GTCTGTGTGTTTCCCTGGTTAC
LOC105337486	CYP17A1-like_6-Forward	GGTAATTGGACGGAACGAGAA
	CYP17A1-like_6-Reverse	GGTTGTGGATTGTGAAGTGGC
LOC105327176	CYP4F22_4-Forward	TGCTGGGACACCTACCACATAT
	CYP4F22_4-Reverse	GTTTTGGATCTGCCGTTCTCA
LOC105326257	BAX1-Forward	TCCACTGGAATATGTTCGAG
	BAX1-Reverse	GAAAGTTTCATGGTTTGCAC
LOC105322048	BI1-Forward	AATGGGCTTCCTGAGGAAGG
	BI1-Reverse	GCAACCAACAGCATCCAGTG
LOC105338957	EF-Forward	AGTCACCAAGGCTGCACAGAAAG
	EF-Reverse	TCCGACGTATTTCTTTGCGATGT

3. Results

3.1. Identification and annotation of CYP genes in the C. gigas

A total of 123 CYP genes were identified in the Pacific oyster genome and 11 CYP genes were renamed according to the nomenclature guidelines (Nelson et al., 2004). Among the 123 identified CYPs, two were pseudogenes, namely CYP 3A4-like_2 (LOC117687834) and CYP3A4-like_5 (LOC117685407). Therefore, further analyses were conducted on the 121 protein-coding genes. The identified *C. gigas* CYPs were divided into five major clans: clan 2, clan 3, clan 4, mitochondrial clan (Mito clan) and others, which were further classified into 16 families (1, 2, 3, 4, 7, 10, 13, 17, 20, 24, 26, 27, 39, 44, 49, 120). Specifically, the 123 *C. gigas* CYPs were composed of approximately 48.0 % genes in clan 2, 14.6 % in clan 3, 12.2% in clan 4, 17.1% in Mito clan, and 8.1 % in others. Among which, clan 2 contained the highest number of CYPs in the *C. gigas*.

3.2. Phylogenetic analyses of CYP genes in the C. gigas

The phylogenetic tree was constructed with 121 CYP protein sequences identified from *C. gigas*, 57 CYP sequences from human, 49 CYP sequences from chicken, 88 CYP sequences from zebrafish and 113 CYP sequences from eastern oyster to reveal the relationship among CYP families in these species.

According to the phylogenetic tree (Fig. 1), five major clans were found in the *C. gigas*, including clan 2, clan 3, clan 4, Mito clan and others. It's apparent that clan 2 was the largest clan and was the ancestor

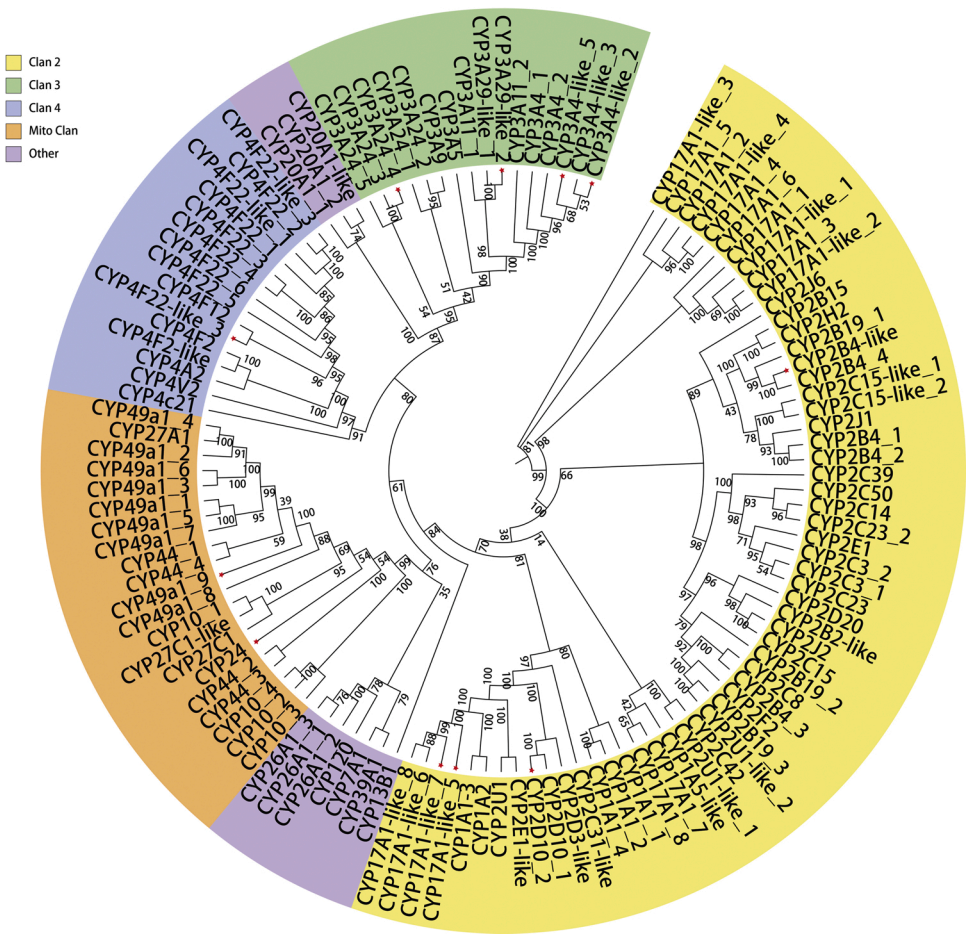

Fig. 1. Phylogenetic analyses of CYP genes. The 121 CYP protein sequences of the *C. gigas* were subject to multiple sequence alignment and phylogenetic analysis using Maximum Likelihood method. CYP clans were represented by different colors. Yellow, green, blue, orange and purple represent clan 2, clan 3, clan 4, Mito clan and other, respectively. The red stars denoted the CYP genes that were reannotated and renamed according to the latest genome annotation and CYP nomenclature guideline (see methods).

of others in the oyster.

3.2.1. CYPs in clan 2 in the C. gigas

According to model test of clan 2 sequences of five species, the LG + R5 model was chosen to generate the phylogenetic tree. The results showed that most CYP families had clear clustering, only few CYP families were mixed (Fig. 2 and Fig. S1). For instance, CYP1A, CYP17A1-like and CYP2 were clustered in a clade. Interestingly, CYP1A-like of Mediterranean mussel were also clustered to CYP2, which may be due to high similarity between the two families or poor genomic annotation. What's more, clan 2 is significantly expanded compared to vertebrates, although it is only composed of CYP1, 2, and 17.

3.2.2. CYPs in clan 3, clan4, Mito clan and others in the C. gigas

According to the phylogenetic analysis (Fig. 3 and Fig. S2), it's clear that all CYP clans were clustered with their counterparts from other species, except CYP4c21-like. As shown in Fig. 3, CYP3A4-like and CYP3A24 possessed multiple copies. Similarly, CYP4F22 in oysters was remarkably duplicated compared with vertebrates, clustered in a single clade. Besides, in vertebrates, clan 4 included only the CYP4 family. The oyster CYP4V2 was clustered with members of human CYP4V, indicating the conservation of functional roles. CYPs in the Mito clan also showed multiple expansions in the *C. gigas*, resulting in species-specific clusters. The Mito clan contains three CYP families in vertebrates, including CYP11, CYP24 and CYP27, while the Mito clan in the *C. gigas* also included CYP10, CYP44 and CYP49. And the members of oyster CYP10 clustered with members of CYP27. Others included clans except for the four clans mentioned above, which shared with vertebrate or plant families (CYP26, CYP7, CYP39, CYP20, CYP13, CYP120), respectively. However, it is noted that the *C. gigas* CYP4C21-like and *C. virginica* CYP4C21-like clustered with CYP3A24.

3.3. Sequence characteristics of CYPs in the C. gigas

The sequence information of 121 CYP genes were presented in the supplementary Table S1, which provided information including gene names, accession numbers, sequence features and genomic locations on the chromosome. The average amino acid number of CYPs was 485, molecular weight (Mw) was 55.7 kDa, and isoelectric point ranged from 5.25 to 9.34. The conserved domain position of CYP was detected on each CYP protein, and few component divergences were presented across diff ;erent members of CYPs.

To further analyze the structural diversity of CYP proteins, the conserved motifs of 121 CYPs were analyzed as shown in Fig. 4. Five conserved motifs were identified from 116 sequences, leaving five CYPs failed to detect all typical motifs which may be due to partial sequences. The length of these motifs varied from 15 to 50 amino acids. The analyses of conserved motifs indicated that *C. gigas* CYP proteins had five basic and relatively conserved motifs that were arranged from the N-terminal to C-terminal as follows: the helix-C motif (WxxxR), the helix I motif (GxE/DTT), the helix K motif (ExxR), the PERF motif (PxRx) and the heme-binding motif (FxxGxRxCxG) (Fig. 4). The most conserved motif was the heme-binding region FxxGxRxCxG (also known as the CxG motif). Among the 121 CYPs identified, 113 had a heme-binding site. The PERF domain (PxRx) is the second conserved motif in the *C. gigas* CYP, in all but six of the *C. gigas* CYPs, a phenylalanine residue was found at the first position. As expected, in the third position, the most common residue was a proline, followed in sequence by a less conserved tyrosine and completely conserved arginine at the fifth position. The third conserved motif is the K-helix domain (ExxR), which is also

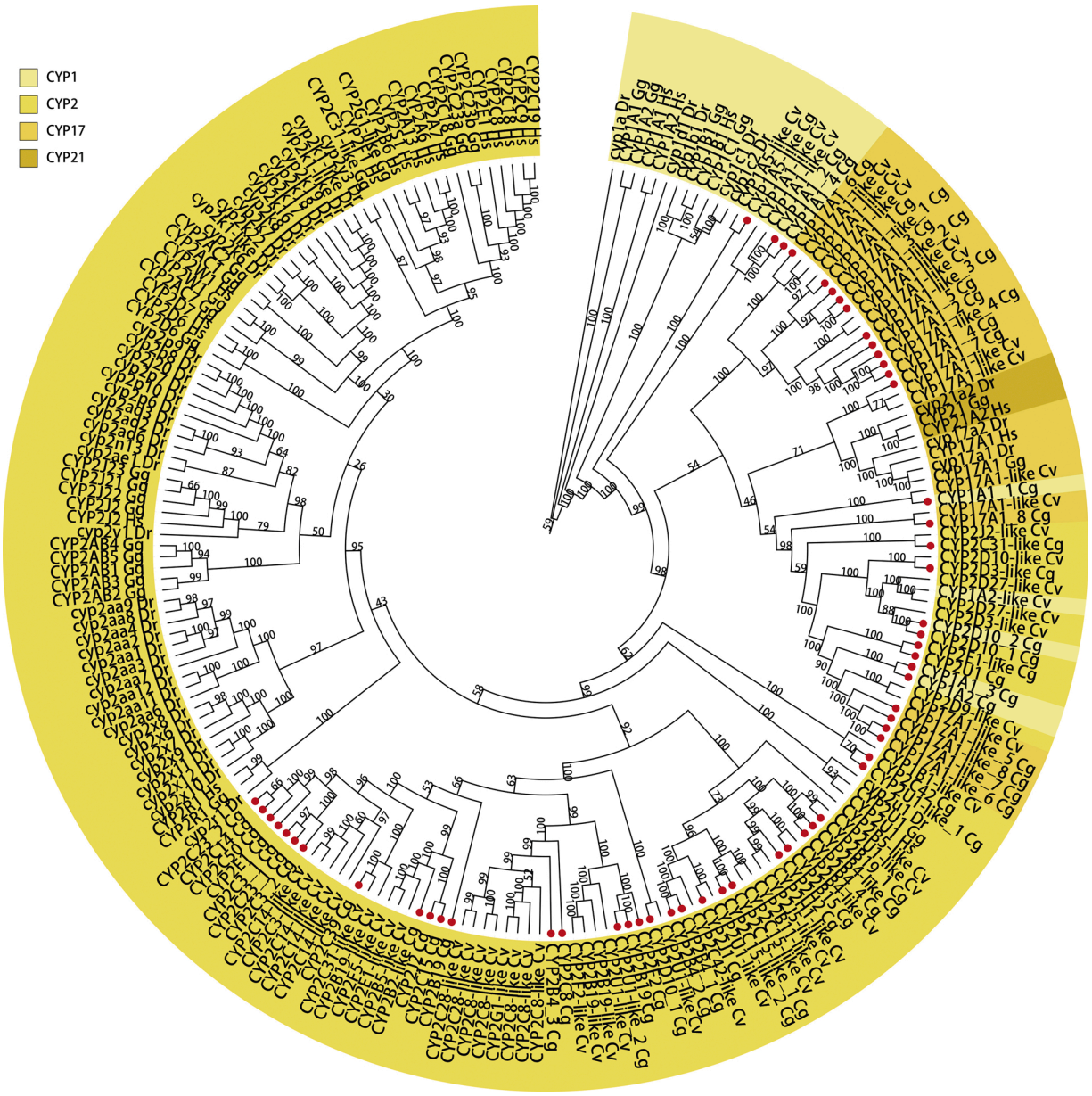

Fig. 2. Phylogenetic analysis of the clan 2 members in the *C. gigas* and four other species. Four other species included *Homo sapiens*, *Danio rerio*, *Gallus gallus*, and *Crassostrea virginica,* with species names being abbreviated as Hs, Dr, Gg, Cv, and Cg, respectively. The red circle denoted the *C. gigas* CYP genes. The bootstrap values (1000 replicates) are shown above the branches.

essential for stabilizing the conserved core structure of CYPs (Sirim et al., 2010). Among the ExxR motifs of the *C. gigas* CYPs, the ETLR was the most abundant pattern. Threonine, valine and Serine were shown to be the most frequent residues at the second position of the ExxR motif in the *C. gigas* CYPs, in agreement with what has been previously reported in fungi (Syed and Mashele, 2014). The next conserved motif, the I-helix domain (AGxDTT), also known as the oxygen-binding domain (OBD), contributes to oxygen binding and activation, with the first (an alanine in most cases), second (a glycine in most cases) and fifth (a threonine in most cases) positions being the most conserved ones. At the fourth position, the most common residues were glutamic acid and aspartic acid, in agreement with some fungal CYPs as reported (Cordova et al., 2017; Hernandez-Martinez et al., 2016). The last conserved motif is C-helix region (WxxxR), the majority of CYP members in clan 2 (except CYP1), clan 3, clan 4 and Mito clan had this WxxxR motif.

3.4. Cd accumulation in tissues of the C. gigas

Distinct pattern of accumulated Cd was observed between the gill and digestive gland of the Pacific oyster (Fig. 5). Cd accumulation in oyster gill increased by 39.3-fold compared to the control (without Cd exposure) after 28 days of exposure. The measured Cd concentration at 28d in the gill was 181 mg/kg (dry weight), as compared to 4.57 mg/kg (dry weight) of the control oysters. In the digestive gland, however, a different pattern was observed. After 7 days of exposure, the Cd concentrations in oyster digestive gland reached to 182.6 mg/kg (dry weight), and increased by 15.7-fold compared with the control. Thereafter, the concentrations of Cd decreased rapidly. Until day 28, the concentration was decreased to 79.7 mg/kg.

3.5. Expression profiling of CYPs after Cd exposure

To obtain insights into the potential roles of CYP in response to

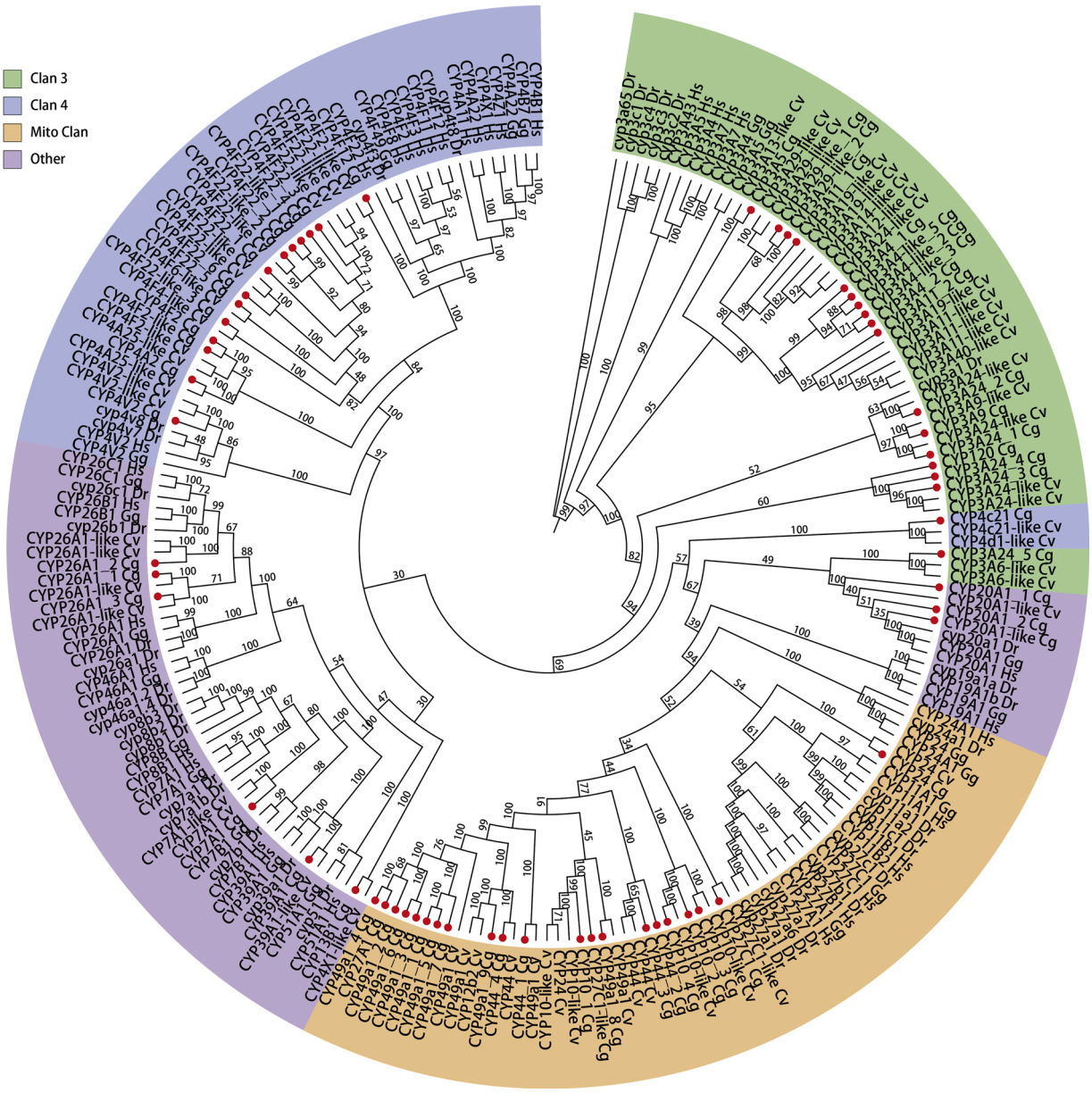

Fig. 3. Phylogenetic analysis of clan 3, clan 4, Mito clan and other in the *C. gigas* and other four species. Four other species included *Homo sapiens*, *Danio rerio*, *Gallus gallus*, and *Crassostrea virginica,* with species names being abbreviated as Hs, Dr, Gg, Cv, and Cg, respectively. The red circle denoted the *C. gigas* CYP genes. The bootstrap values (1000 replicates) are shown above the branches.

cadmium exposure, we examined the expression profiles of 14 CYP genes that were selected based on the meta-analysis of the publicly available RNA-seq datasets (Meng et al., 2017). Since the time-point 7d was close to the time-point 9d of the transcriptome data for meta-analysis, we first determined the relative expression of 14 genes in the samples collected on the 7d during the experiment (Fig. 6). In the gill, the expression levels of CYP17A1_3, CYP4V2 and CYP4F22_4, were significantly upregulated after Cd exposure at the 7d (Fig. 6A). While in the digestive gland, CYP17A1-like_6 and CYP2C50 were significantly upregulated (Fig. 6B).

Based on the results of cadmium content in gill and digestive gland, we speculate that the digestive gland would be the major place to participate in detoxification in the *C. gigas*. Based on this speculation, we selected four CYPs (CYP17A1-like_6, CYP2C50, CYP24 and CYP1A1_4) for further expression analyses at more time points in the digestive gland. As shown in Fig. 7A, the expression pattern was highly consistent with that of the Cd content. The CYP17A1-like_6 and CYP2C50 mRNA levels were significantly increased on the 7th day when the cadmium content was also at a high level, suggesting the organism responded to the Cd when being accumulated to a certain extent. After day 14, the cadmium content was decreased gradually, while the expression levels of CYP17A1-like_6 and CYP2C50 were also regulated to the control level. On day 28, the expression of the genes was significantly suppressed, suggesting their critical roles involved in the detoxification process. As the Cd cytotoxicity could lead to apoptosis and necrosis. We verified the relative expression of two apoptosis-associated genes, Bax inhibitor 1 (BI1) and BAX1 at various time points in oyster digestive gland after Cd exposure. Interestingly, the results showed that BI1 and BAX1 exhibited the same expression trend. From day 14 to day 28, the expression level returned to the control level (Fig. 7B).

4. Discussion

Heavy metal pollution has become an important environmental

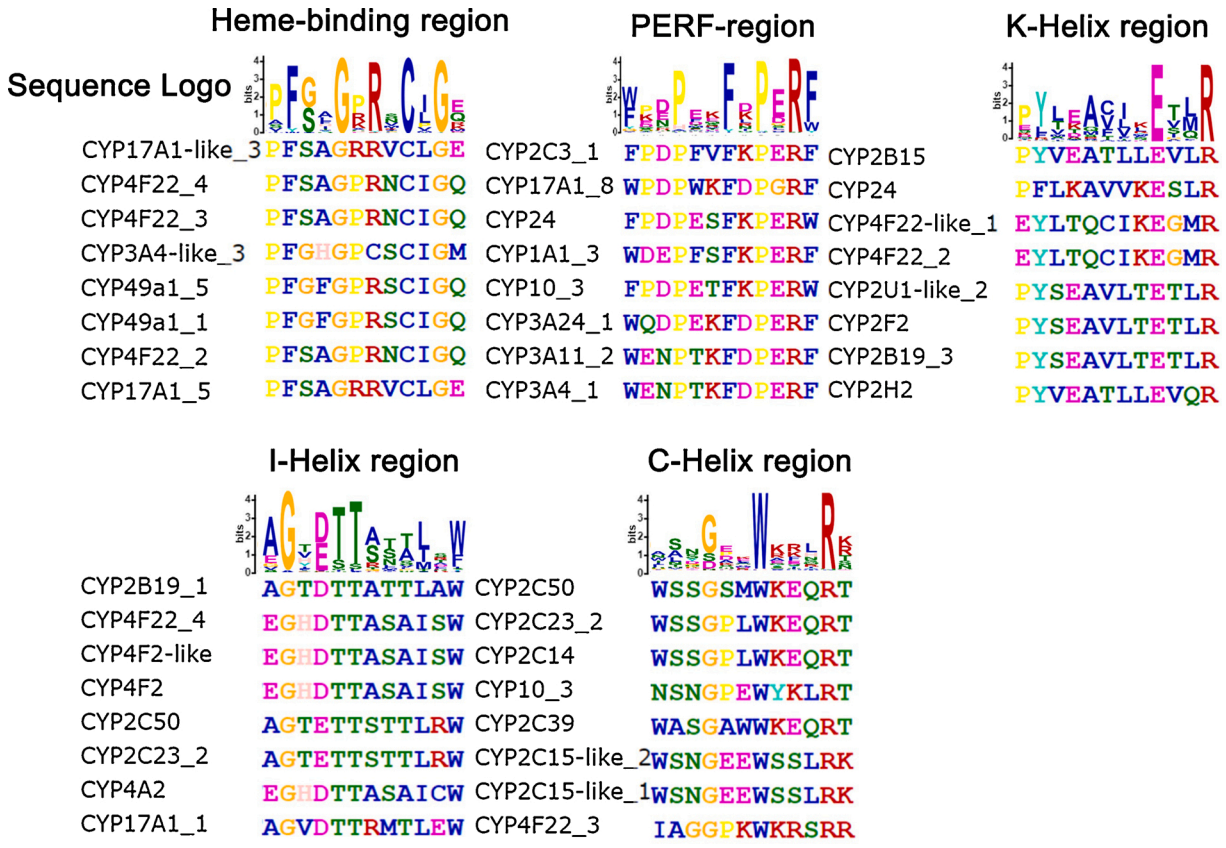

Fig. 4. Five most conserved motifs in the CYP proteins of the *C. gigas*. The height of a letter indicates its relative frequency at the given position for the amino acid. The conserved motifs from left to right is Heme-binding region (FxxGxRxCxG), PERF motif region (PxRx), K-helix region (ExxR), I-helix region (GxE/DTT) and C-helix region (WxxxR). Each motif is represented by multiple alignments of randomly selected representative CYP sequences.

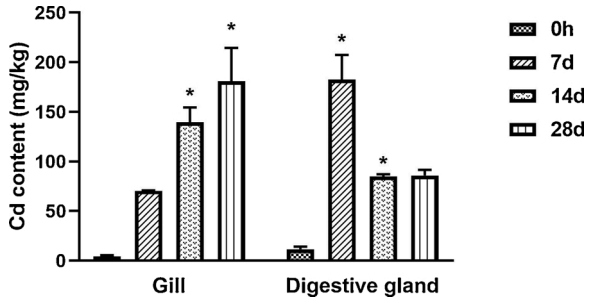

Fig. 5. Cd contents in the oyster gill and digestive gland at different time points after Cd exposure. Asterisk (*) indicates significant differences compared with 0 h time point (mean ± S.D; N = 3, ANOVA, $P < 0.05$).

threat to oceans all over the world. Shellfish, especially oysters, have a strong ability to accumulate heavy metals, causing serious aquatic product safety problems. It's reported that the highest level of zinc in some contaminated oysters was about 120 mg/g dry weight, about 12 percent of soft tissue weight, which may be the highest recorded in all organisms (Wang et al., 2018). The analysis of the accumulation mechanism of heavy metals in oyster will be valuable to solve the food safety problem.

Cytochrome P450s (CYPs), as an important first-phase detoxifying enzyme, are found in almost all aerobic organisms. Detoxification of toxic substances such as aromatic hydrocarbons, pesticides, and heavy metals has been shown to be essential in many species (He et al., 2019; Lu et al., 2020; Prasad et al., 2015; Zhang et al., 2019). Uncovering additional information about CYP allows for understanding of metabolic mechanisms of toxic substances. Therefore, systematic characterization and expression profiling of CYPs after exposure to heavy metals would be of great interest to the research community. In this study, we identified a full-set of 123 CYP genes in the *C. gigas* based on bioinformatics analyses of multiple omics data resources. The number of CYP genes identified in the *C. gigas* is greater than that of other animals such as *Chlamys farreri* with 88 CYP genes, *Tigriopus japonicus* with 52 CYPs, *Drosophila melanogaster* with 85 CYPs, *Danio rerio* with 94 CYPs and *Homo sapiens* with 57 CYP genes. Our analyses showed an expansion of the *C. gigas* CYP family, which could contribute to diversity of the CYPs that are involved in many complex metabolic processes in the *C. gigas* (Goldstone et al., 2010; Guo et al., 2012; Han et al., 2017).

The phylogenetic analyses revealed clan 2 and Mito clan are the two largest of five clans in the *C. gigas*, which was consistent with observation in previous studies. The genome annotation has shown that CYP expanded significantly in the *C. gigas*, especially the CYP2 family (Zhang et al., 2012). In human, the CYP members in clan 2 were mainly involved in the metabolism of xenobiotics, drugs and steroids. Significant expansion of clan 2 CYPs may be closely related to the detoxification of similar xenobiotics. Mito clan was named by their subcellular locations (Nebert et al., 1991). The *C. gigas* Mito clan included families that are specific to other organisms. Specifically, in addition to CYP24 and 27 families, the *C. gigas* also possessed CYP10, CYP44 and CYP49 families, which were specifically identified in Zhikong scallop, copepod and diamondback moth, respectively (Guo et al., 2012; Han et al., 2017; Yu et al., 2015). These observations indicated that new functions of CYPs may have been gained in response to environmental changes. Generally, evolutionary diversification of individual CYP clans could be one of the outcomes of adaptation to natural and synthetic environmental factors (Berenbaum, 2002).

Motif analyses revealed that the *C. gigas* CYPs have typical CYP family domains, such as helix-C, helix-I, helix-K, PERF and heme-

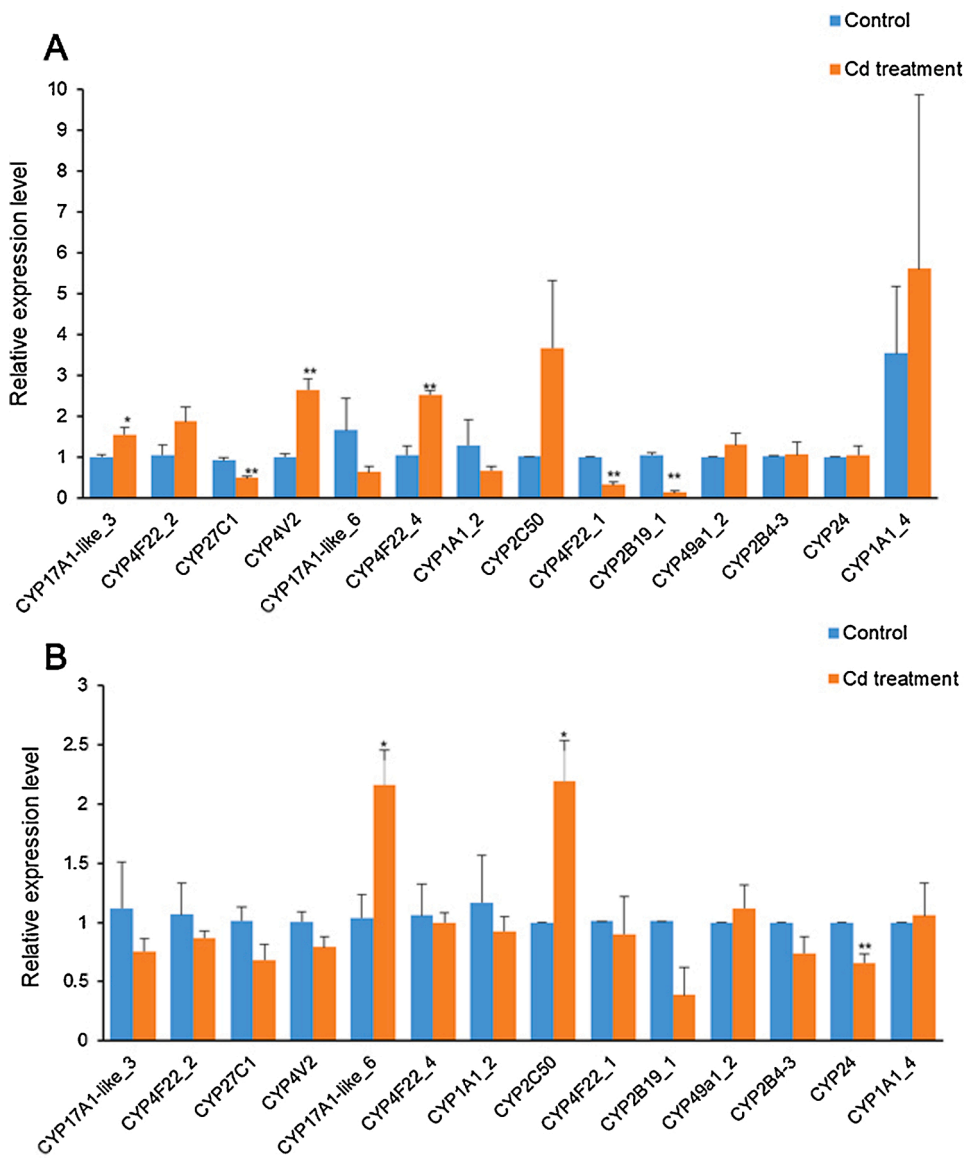

Fig. 6. Expression profiles of 14 CYP genes in different tissues after 7d Cd exposure. (A) Relative expression level of 14 CYPs in the gill; (B) Relative expression level of 14 CYPs in the digestive gland. The statistical analysis was performed using ANOVA and Dunnett's two-tailed *t*-test. Values are shown as mean ± S.E. Significant difference compared to the control expression level was marked with asterisks (* $0.01<P<0.05$; ** $P<0.01$).

binding domains, indicating that CYP450 superfamily is conserved in most organisms (Fig. 4). The cysteine heme-binding domain of CYPs is highly conserved and used to identify CYPs in diverse organisms such as bacteria, animals, and plants, which is involved in the electron-transport pathway ($NADPH^{-}$ to NADP) that plays a crucial role in oxidative hydroxylation reaction (Nelson, 1999; Otyepka et al., 2007; Saxena et al., 2013; Werck-Reichhart and Feyereisen, 2000). It has been reported that arginine is the predominant residue at the sixth position of the FxxGxRxCxG motif, and this is the case in all of the *C. gigas* CYPs except for CYP3A4-like_3, CYP4c21-like, CYP39A1 and CYP26A1_1. For the CxG pattern (the last three residues of the FxxGxRxCxG motif), the three with the highest frequency are CIG, CLG and CPG pattern. Although the effect of the different amino acids in the middle position of the triad CxG is still unknown, previous studies have demonstrated that different CYP families show preference for determined residues at this position, suggesting that amino acids in this motif play a role in determining CYP structure, activity and substrate specificity (Syed and Mashele, 2014). Besides, PERF is important for locking the structure of the heme pocket in place and ensuring the stabilization of the core structure (Cordova et al., 2017). Although PERF has four amino acids, the two previous residues were also considered in the analysis, giving a six-amino-acid sequence, as a phenylalanine residue two positions before the conserved proline of the PxRx motif is highly conserved in most CYPs (Chen et al., 2014). In addition to the conserved typical motifs of CYP genes investigated, the promoter regions of two up-regulated CYPs contain metal response elements (MRE) like sequences, cis-acting DNA elements that specifically bind metal transcription factor (MTF1). This unique gene structure may be associated with expression regulation of CYPs in response to metal stress, which deserves future investigations.

Metal bioaccumulation is specific for different pollutants and animal species. The capacity to accumulate high levels of metals in oysters is an interesting evolutionary phenomenon. Oysters not only are able to survive in highly metal-contaminated environments, but also can accumulate metals to extremely high levels without obvious toxic effects. In our results, it's clear that the maximum cadmium content was observed in the digestive gland compared to the gill. In a previous study, the digestive gland was proved to be the major tissue for heavy metal accumulation, with more differentially expressed genes being identified

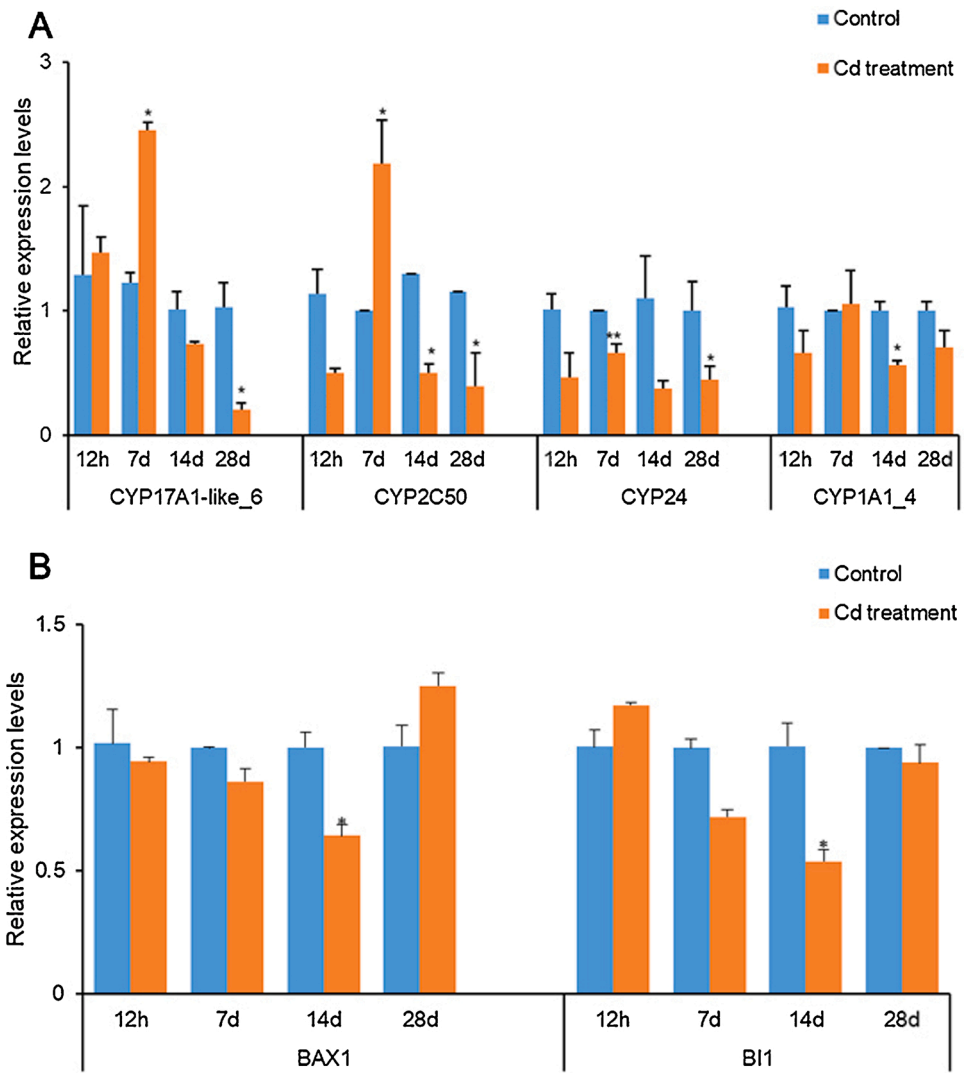

Fig. 7. Expression profiles of four CYP genes and two representative apoptosis genes. (A) Four CYP genes (B) Two apoptosis-related genes. The statistical analysis was performed using ANOVA and Dunnett's two-tailed *t*-test. Values are shown as mean ± S.E. Significant difference compared to the control expression level at the same sampling time was marked with asterisks (* $0.01<P<0.05$; ** $P<0.01$).

in the digestive gland than the gill after heavy metal exposure (Meng et al., 2017). Moreover, the contents of the two tissues showed different trends at different time points. Previous studies have shown that the accumulation of Cd in oyster gill and visceral mass showed a similar increasing pattern. After exposure to 100 μg/L Cd, they found that the accumulation rate of heavy metal in oysters increased significantly after day 9, and reached to the highest level on day 13, with over 10 times higher level than that of the control group (Meng et al., 2017). However, our results showed that cadmium content in the digestive gland decreased significantly after reaching its maximum value on day 7, suggesting that the digestive gland appears to act as a major detoxifying site. The gill has been regarded as the major tissue of the bivalve to exchange the hydrotropic metal ions, but might play a major defensive role in an acute stress (Luo et al., 2014).

Transcriptional upregulation of CYP genes is considered as an important indicator for biological monitoring of exposure to marine pollutants because CYP-dependent xenobiotic metabolism is the first-line detoxification or biotransformation mechanism in diverse living organisms. We first determined the expression of 14 CYPs in the gill and digestive gland on day 7 of the experiment, and found the difference of CYP expression between the two tissues, indicating the distinct detoxification mechanism in the two tissues. According to the changes of cadmium content in digestive gland, we speculated that the upregulated CYP was corresponding to the increase of cadmium content on the 7th day. Thus, the relative expression of four CYPs (CYP17A1-like_6, CYP2C50, CYP24 and CYP1A1_4) in the digestive gland were performed at different time points. We included CYP1A1_4 for further expression analysis because it was previously reported to be involved in detoxification of xenobiotic substances such as PAH (Li et al., 2013; Shimada et al., 2001). The results showed that the expression of CYP17A1-like_6 and CYP2C50 at four time points in the digestive gland was consistent with changing trend of cadmium content. Interestingly, the expression of four CYPs were suppressed at day 28 compared with the control group. The potential explanation lies in three aspects (Fig. 8):

(1) From Cd contents perspective, when the content of cadmium in digestive gland reached its maximum value on day 7, the relative expression level of CYP increased significantly, which might play a role in metabolism and biotransformation. The content of cadmium in digestive gland was still higher than that in the control group on day 28, even though there were no significant statistical difference. Therefore, the significant decrease in the relative expression of CYP on day 28 could be due to the organismal homeostasis regulation, through suppression the expression

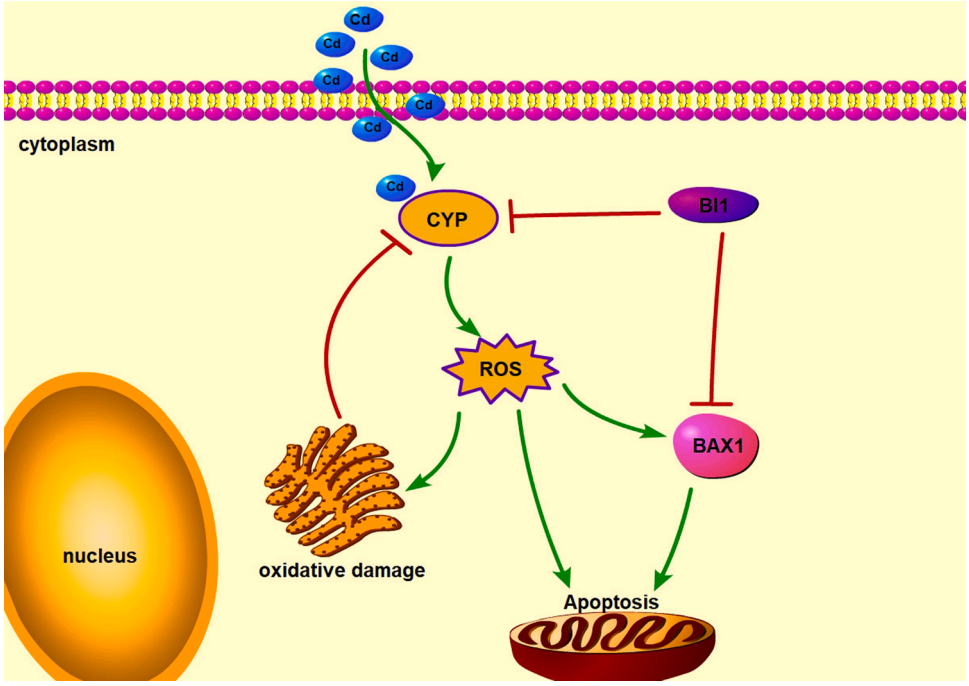

Fig. 8. Hypothesis model for CYPs involved in Cd detoxification in the *C. gigas*. In oysters, CYPs can directly or indirectly metabolize Cd and generate ROS. Enhanced expression of CYPs could be subject to suppression to reduce oxidative damage caused by ROS. Overexpression of CYP could induce apoptosis process, which is under regulation by critical apoptosis-associated genes (i.e., *BI1* and *BAX1*) to maintain homeostasis of apoptosis.

to reduce oxidative damage. Previous studies have shown that overexpression of CYP can lead to the production of ROS, thus causing oxidative damage to the body. Decreased expression of CYP may be associated with the ROS and prevention of oxidative stress (Benedetti et al., 2007; Binda et al., 2003). Meng et al. (2017) reported that ROS production increased significantly after 9 days of Cd exposure as compared to the control. Studies indicated that ROS have been shown to play a role in the decrease of CYP in vivo and in vitro, an effect that is modulated by changing its cellular redox potential (Elbekai and El-Kadi, 2005). It has also been reported that CYP1A genes are associated with oxidative stress and accumulation of mRNA is prevented by ROS at the transcriptional level (Barouki and Morel, 2001). Therefore, prevention of damage caused by metal stress may due to its flexible self-regulation capacity.

(2) CYP levels might affect various signal transduction pathways that alter the cell cycle, causing apoptosis or aberrant cell growth (Nebert and Dalton, 2006; Zhang et al., 2018). The consequences of Cd cytotoxicity involve apoptosis and necrosis. Liu and Baliga (2003) demonstrated the pivotal role of CYP2E1 in cisplatin-induced nephrotoxicity and apoptosis. Similarly, Kim et al. (2009) found that overexpression of anti-apoptotic protein Bax inhibitor 1 (BI1) reduced the interaction between NADPH-P450 reductase (NPR) and CYP2E1, and decreased the catalytic activity of CYP2E1. Therefore, there might exist a certain relationship between cadmium, CYP, and apoptosis in oysters. A previous study (Rolland et al., 2014) reported a feedback mechanism, which may occur in the digestive gland of the Pacific oyster where BI-1 could play a key role in preventing the induction of apoptosis by PSTs (paralytic shellfish toxins) through inhibiting Bax and limiting CYP1A converting PSTs to ROS. Thus, we speculated that BI regulated CYP expression in this way and verified the relative expression of BI1 and BAX1 at various time-points in oyster digestive gland. Interestingly, our results showed that BAX1 and BI1 exhibited the same expression trend (Fig. 7B). From day 14 to day 28, the expression level returned to the control level. Therefore, the decreased expression of CYP on day 28 may be due to the increased expression of BI1 between day 14 and 28 to reduce the accumulation of ROS produced by CYP overexpression. This may also be a feedback mechanism in oysters under heavy metal stress.

(3) CYP expression was affected by many other factors. Many studies reported that treatment concentration, treatment time, developmental stage and specific tissue of the subject also affected CYP expression (Han et al., 2017). Therefore, the significant decreased expression of these CYPs on day 28 may be influenced by a variety of factors, which is involved in a complicated process.

Owing to the complexity of CYP family and the substrate specificity of each member, the expression patterns of CYP under cadmium stress are highly diverse and variable. For down-regulated CYPs, we hypothesized that those CYP genes may be affected by metal exposure, such as oxidative stress, which in turn affects CYP-mediated biological processes. It's reported that ROS generated by metals plays a role in the decreased levels of CYP450 in vivo and in vitro (Elbekai and El-Kadi, 2004). Expression of CYPs can affect the production of molecules derived from arachidonic acid, and alters various downstream signal-transduction pathways (Nebert and Dalton, 2006). However, the up-regulated CYPs were likely associated with the detoxification processes. Our results suggested that the up-regulated CYP17A1-like_6 and CYP2C50 might play critical roles upon Cd exposure, which required further functional investigations.

5. Conclusions

We identified a total of 123 CYP genes in the *C. gigas*. The CYPs exhibited tissue-specific expression patterns in the *C. gigas* after Cd exposure. The significantly higher expression levels of CYP17A1-like_6 and CYP2C50 in response to Cd exposure, suggesting their potential involvement in heavy metal metabolism and detoxification. To the best of our knowledge, this work presented the first comprehensive analysis of CYP genes in the Pacific oyster. The information should be valuable

for better understanding of CYP function and set the foundation for future study on the molecular mechanism of heavy metals detoxification in bivalves.

CRediT authorship contribution statement

Jing Tian: Investigation, Data curation, Writing - original draft. **Zexin Jiao:** Data curation. **Huiru Fu:** Methodology. **Lu Qi:** Methodology, Software. **Qi Li:** Supervision, Resources. **Nannan Liu:** Data curation. **Shikai Liu:** Supervision, Data curation, Resources, Writing - review & editing.

Declaration of Competing Interest

The authors declare that they have no known competing financial interests or personal relationships that could have appeared to influence the work reported in this paper.

Acknowledgements

This work was supported by the grants from National Natural Science Foundation of China (Nos. 31802293 and 41976098), the Young Talent Program of Ocean University of China (No. 201812013) and the Ocean University of China-Auburn University Joint Research Center for Aquaculture and Environmental Science (No. 861901154277).

Appendix A. Supplementary data

Supplementary material related to this article can be found, in the online version, at doi:https://doi.org/10.1016/j.aqrep.2020.100582.

References

Abu-Bakar, A., Satarug, S., Marks, G.C., Lang, M.A., Moore, M.R., 2004. Acute cadmium chloride administration induces hepatic and renal CYP2A5 mRNA, protein and activity in the mouse: involvement of transcription factor NRF2. Toxicol. Lett. 148, 199–210.

Alfonso, J.A., Handt, H., Mora, A., Vasquez, Y., Azocar, J., Marcano, E., 2013. Temporal distribution of heavy metal concentrations in oysters *Crassostrea rhizophorae* from the central Venezuelan coast. Mar. Pollut. Bull. 73, 394–398.

Anders, S., Huber, W., 2010. Differential expression analysis for sequence count data. Genome Biol. 11 (10), R106.

Baldwin, W.S., Marko, P.B., Nelson, D.R., 2009. The cytochrome P450 (CYP) gene superfamily in *Daphnia pulex*. BMC Genomics 10, 169.

Barouki, R., Morel, Y., 2001. Repression of cytochrome P450 1A1 gene expression by oxidative stress: mechanisms and biological implications. Biochem. Pharmacol. 61, 511–516.

Benedetti, M., Martuccio, G., Fattorini, D., Canapa, A., Barucca, M., Nigro, M., Regoli, F., 2007. Oxidative and modulatory effects of trace metals on metabolism of polycyclic aromatic hydrocarbons in the Antarctic fish Trematomus bernacchiile. Aquat. Toxicol. 85, 167–175.

Berenbaum, M.R., 2002. Postgenomic chemical ecology: from genetic code to ecological interactions. J. Chem. Ecol. 28, 873–896.

Binda, D., Lasserre-Bigot, D., Bonet, A., Thomassin, M., Come, M.P., Guinchard, C., Bars, R., Jacqueson, A., Richert, L., 2003. Time course of cytochromes P450 decline during rat hepatocyte isolation and culture: effect of L-NAME. Toxicol. In Vitro 17, 59–67.

Boutet, I., Tanguy, A., Moraga, D., 2004. Response of the Pacific oyster Crassostrea gigas to hydrocarbon contamination under experimental conditions. Gene 329, 147–157.

Brown, P., Baxter, L., Hickman, R., Beynon, J., Moore, J.D., Ott, S., 2013. MEME-LaB: motif analysis in clusters. Bioinformatics 29, 1696–1697.

Castresana, J., 2000. Selection of conserved blocks from multiple alignments for their use in phylogenetic analysis. Mol. Biol. Evol. 17, 540–552.

Chen, Y.Y., Chan, K.M., 2018. Modulations of TCDD-mediated induction of zebrafish cyp1a1 and the AHR pathway by administering $Cd^{(2+)}$in vivo. Chemosphere 210, 577–587.

Chen, W.P., Lee, M.K., Jefcoate, C., Kim, S.C., Chen, F.S., Yu, J.H., 2014. Fungal cytochrome P450 monooxygenases: their distribution, structure, functions, family expansion, and evolutionary origin. Genome Biol. Evol. 6, 1620–1634.

Cong, Y., Chi, Q., Teng, X., Li, S., 2019. The protection of selenium against cadmium-induced mitochondrial damage via the cytochrome P450 in the livers of chicken. Biol. Trace Elem. Res. 190, 484–492.

Cordova, P., Gonzalez, A.M., Nelson, D.R., Gutierrez, M.S., Baeza, M., Cifuentes, V., Alcaino, J., 2017. Characterization of the cytochrome P450 monooxygenase genes (P450ome) from the carotenogenic yeast *Xanthophyllomyces dendrorhous*. BMC Genomics 18, 540.

Elbekai, R.H., El-Kadi, A.O.S., 2004. Modulation of aryl hydrocarbon receptor-regulated gene expression by arsenite, cadmium, and chromium. Toxicology 202, 249–269.

Elbekai, R.H., El-Kadi, A.O.S., 2005. The role of oxidative stress in the modulation of aryl hydrocarbon receptor-regulated genes by As^{3+}, Cd^{2+}, and Cr^{6+}. Free Radical Bio. Med. 39, 1499–1511.

Funes, V., Alhama, J., Navas, J.I., Lopez-Barea, J., Peinado, J., 2006. Ecotoxicological effects of metal pollution in two mollusc species from the Spanish South Atlantic littoral. Environ. Pollut. 139, 214–223.

Garber, M., Grabherr, M.G., Guttman, M., Trapnell, C., 2011. Computational methods for transcriptome annotation and quantification using RNA-seq. Nat. Methods 8, 469–477.

Gawenis, L.R., Stien, X., Shull, G.E., Schultheis, P.J., Woo, A.L., Walker, N.M., Clarke, L. L., 2002. Intestinal NaCl transport in NHE2 and NHE3 knockout mice. Am. J. Physiol. Gastrointest. Liver Physiol. 282, G776–784.

Goldstone, J.V., McArthur, A.G., Kubota, A., Zanette, J., Parente, T., Jonsson, M.E., Nelson, D.R., Stegeman, J.J., 2010. Identification and developmental expression of the full complement of Cytochrome P450 genes in Zebrafish. BMC Genomics 11, 643.

Guo, H., Bao, Z., Du, H., Zhang, L., Wang, S., Sun, L., Mou, X., Hu, X., 2012. Identification of Cytochrome P450 (CYP) genes in Zhikong scallop (*Chlamys farreri*). J. Ocean. Univ. China 12, 97–102.

Han, J., Kim, D.H., Kim, H.S., Nelson, D.R., Lee, J.S., 2017. Genome-wide identification of 52 cytochrome P450 (CYP) genes in the copepod *Tigriopus japonicus* and their B [alpha]P-induced expression patterns. Comp. Biochem. Physiol. Part D Genomics Proteomics 23, 49–57.

He, T.T., Zhang, T., Liu, S.B., Shi, J.C., Huang, Y.S., Zheng, H.P., Liu, W.H., 2019. Toxicological effects benzotriazole to the marine scallop *Chlamys nobilis*: a 2-month exposure study. Environ. Sci. Pollut. Res. Int. 26, 10306–10318.

Hernandez-Martinez, F., Briones-Robler, C.I., Nelson, D.R., Rivera-Orduna, F.N., Zuniga, G., 2016. Cytochrome P450 complement (CYPome) of *Candida oregonensis*, a gut-associated yeast of bark beetle, *Dendroctonus rhizophagus*. Fungal Biol-Uk 120, 1077–1089.

Hillis, D.M., Bull, J.J., 1993. An empirical test of bootstrapping as a method for assessing confidence in phylogenetic analysis. Syst. Biol. 42, 182–192.

Huang, C.C., Kuo, C.Y., Yang, C.Y., Liu, J.M., Hsu, R.J., Lee, K.I., Su, C.C., Wu, C.C., Lin, C.T., Liu, S.H., Huang, C.F., 2019. Cadmium exposure induces pancreatic beta-cell death via a $Ca^{(2+)}$-triggered JNK/CHOP-related apoptotic signaling pathway. Toxicology 425, 152252.

Katoh, K., Misawa, K., Kuma, K., Miyata, T., 2002. MAFFT: a novel method for rapid multiple sequence alignment based on fast Fourier transform. Nucleic Acids Res. 30, 3059–3066.

Kim, H.R., Lee, G.H., Cho, E.Y., Chae, S.W., Ahn, T., Chae, H.J., 2009. Bax inhibitor 1 regulates ER-stress-induced ROS accumulation through the regulation of cytochrome P450 2E1. J. Cell. Sci. 122, 1126–1133.

Kim, D., Langmead, B., Salzberg, S.L., 2015. HISAT: a fast spliced aligner with low memory requirements. Nat. Methods 12, 357–360.

Korashy, H.M., El-Kadi, A.O., 2004. Differential effects of mercury, lead and copper on the constitutive and inducible expression of aryl hydrocarbon receptor (AHR)-regulated genes in cultured hepatoma Hepa 1c1c7 cells. Toxicology 201, 153–172.

Larigot, L., Juricek, L., Dairou, J., Coumoul, X., 2018. AhR signaling pathways and regulatory functions. Biochim. Open 7, 1–9.

Li, G.Y., Shen, D., Liang, X.F., He, Y., He, S., 2013. Effects of malachite green on the mRNA expression of detoxification-related genes in Nile Tilapia (*Oreochromis niloticus*) and other major chinese freshwater fishes. Environ. Toxicol. 28, 137–145.

Liu, H., Baliga, R., 2003. Cytochrome P450 2E1 null mice provide novel protection against cisplatin-induced nephrotoxicity and apoptosis. Kidney Int. 63, 1687–1696.

Liu, N.N., Li, M., Gong, Y.H., Liu, F., Li, T., 2015. Cytochrome P450s-Their expression, regulation, and role in insecticide resistance. Pestic. Biochem. Phys. 120, 77–81.

Liu, G., Tian, J., Yin, H., Yin, J., Tang, Y., 2019. Self-protective transcriptional alterations in ZF4 cells exposed to Pb(NO3)2 and AgNO3. J. Biochem. Mol. Toxicol. 33, e22408.

Livingstone, D.R., Lips, F., Martinez, P.G., Pipe, R.K., 1992. Antioxidant enzymes in the digestive gland of the common mussel *mytilus-edulis*. Mar. Biol. 112, 265–276.

Lu, K., Cheng, Y., Li, W., Li, Y., Zeng, R., Song, Y., 2020. Activation of CncC pathway by ROS burst regulates cytochrome P450 CYP6AB12 responsible for lambda-cyhalothrin tolerance in *Spodoptera litura*. J. Hazard. Mater. 387, 121698.

Luo, L., Ke, C., Guo, X., Shi, B., Huang, M., 2014. Metal accumulation and differentially expressed proteins in gill of oyster (*Crassostrea hongkongensis*) exposed to long-term heavy metal-contaminated estuary. Fish Shellfish Immunol. 38, 318–329.

Meng, J., Wang, W., Li, L., Yin, Q., Zhang, G., 2017. Cadmium effects on DNA and protein metabolism in oyster (*Crassostrea gigas*) revealed by proteomic analyses. Sci. Rep. 7, 11716.

Meng, J., Wang, W.X., Li, L., Zhang, G., 2018. Tissue-specific molecular and cellular toxicity of Pb in the oyster (*Crassostrea gigas*): mRNA expression and physiological studies. Aquat. Toxicol. 198, 257–268.

Nebert, D.W., Dalton, T.P., 2006. The role of cytochrome P450 enzymes in endogenous signalling pathways and environmental carcinogenesis. Nat. Rev. Cancer 6, 947–960.

Nebert, D.W., Adesnik, M., Coon, M.J., Estabrook, R.W., Gonzalez, F.J., Guengerich, F.P., Gunsalus, I.C., Johnson, E.F., Kemper, B., Levin, W., et al., 1987. The P450 gene superfamily: recommended nomenclature. DNA 6, 1–11.

Nebert, D.W., Nelson, D.R., Coon, M.J., Estabrook, R.W., Feyereisen, R., Fujiikuriyama, Y., Gonzalez, F.J., Guengerich, F.P., Gunsalus, I.C., Johnson, E.F., Loper, J.C., Sato, R., Waterman, M.R., Waxman, D.J., 1991. The P450 superfamily - update on new sequences, gene-mapping, and recommended nomenclature. DNA Cell Biol. 10, 1–14.

Nelson, D.R., 1999. Cytochrome P450 and the individuality of species. Arch. Biochem. Biophys. 369, 1–10.

Nelson, D.R., Zeldin, D.C., Hoffman, S.M., Maltais, L.J., Wain, H.M., Nebert, D.W., 2004. Comparison of cytochrome P450 (CYP) genes from the mouse and human genomes, including nomenclature recommendations for genes, pseudogenes and alternative-splice variants. Pharmacogenetics 14, 1–18.

Nguyen, L.T., Schmidt, H.A., von Haeseler, A., Minh, B.Q., 2015. IQ-TREE: a fast and effective stochastic algorithm for estimating maximum-likelihood phylogenies. Mol. Biol. Evol. 32, 268–274.

O'Connor, T.P., 2002. National distribution of chemical concentrations in mussels and oysters in the USA. Mar. Environ. Res. 53, 117–143.

Otyepka, M., Skopalik, J., Anzenbacherova, E., Anzenbacher, P., 2007. What common structural features and variations of mammalian P450s are known to date? Biochim. Biophys. Acta 1770, 376–389.

Pan, J., 2015. Single and Combined Effects of Mercury and Cadmium on Mussel *Mytilus edulis*. Ocean University of China, pp. 1–45.

Pan, L.Q., Liu, N., Xu, C.Q., Miao, J.J., 2011. Identification of a novel P450 gene belonging to the CYP4 family in the clam *Ruditapes philippinarum*, and analysis of basal- and benzo(a)pyrene-induced mRNA expression levels in selected tissues. Environ. Toxicol. Pharm. 32, 390–398.

Pertea, M., Pertea, G.M., Antonescu, C.M., Chang, T.C., Mendell, J.T., Salzberg, S.L., 2015. StringTie enables improved reconstruction of a transcriptome from RNA-seq reads. Nat. Biotechnol. 33, 290–295.

Pertea, M., Kim, D., Pertea, G.M., Leek, J.T., Salzberg, S.L., 2016. Transcript-level expression analysis of RNA-seq experiments with HISAT, StringTie and Ballgown. Nat. Protoc. 11, 1650–1667.

Porte, C., Biosca, X., Sole, M., Albaiges, J., 2001. The integrated use of chemical analysis, cytochrome P450 and stress proteins in mussels to assess pollution along the Galician coast (NW Spain). Environ. Pollut. 112, 261–268.

Poteat, M.D., Garland, T., Fisher, N.S., Wang, W.X., Buchwalter, D.B., 2013. Evolutionary patterns in trace metal (Cd and Zn) efflux capacity in aquatic organisms. Environ. Sci. Technol. 47, 7989–7995.

Prasad, M., Rai, A., Singh, R., Shirke, P.A., Tripathi, R.D., Trivedi, P.K., Chakrabarty, D., 2015. Expression of rice CYP450-Like gene (Os08g01480) in Arabidopsis modulates regulatory network leading to heavy metal and other abiotic stress tolerance. PLoS One 10 (9), e0138574.

Rolland, J.L., Medhioub, W., Vergnes, A., Abi-Khalil, C., Savar, V., Abadie, E., Masseret, E., Amzil, Z., Laabir, M., 2014. A feedback mechanism to control apoptosis occurs in the digestive gland of the oyster *Crassostrea gigas* exposed to the paralytic shellfish toxins producer *Alexandrium catenella*. Mar. Drugs 12, 5035–5054.

Saxena, A., Singh, P., Yadav, D.K., Sharma, P., Alam, S., Khan, F., Thul, S.T., Shukla, R.K., Gupta, V., Sangwan, N.S., 2013. Identification of cytochrome P450 heme motif in plants proteome. Plant Omics 6, 1–12.

Shimada, T., Oda, Y., Gillam, E.M., Guengerich, F.P., Inoue, K., 2001. Metabolic activation of polycyclic aromatic hydrocarbons and other procarcinogens by cytochromes P450 1A1 and P450 1B1 allelic variants and other human cytochromes P450 in *Salmonella typhimurium* NM2009. Drug Metab. Dispos. 29, 1176–1182.

Sirim, D., Widmann, M., Wagner, F., Pleiss, J., 2010. Prediction and analysis of the modular structure of cytochrome P450 monooxygenases. BMC Struct. Biol. 10, 34.

Sun, M., Liu, G., Lin, H., Zhang, T., Guo, W., 2018. Effect of salinity on the bioaccumulation and depuration of cadmium in the Pacific cupped oyster, *Crassostrea gigas*. Environ. Toxicol. Pharmacol. 62, 88–97.

Syed, K., Mashele, S.S., 2014. Comparative analysis of P450 signature motifs EXXR and CXG in the large and diverse kingdom of fungi: identification of evolutionarily conserved amino acid patterns characteristic of P450 family. PLoS One 9 (4), e95616.

Tian, S., Pan, L., Zhang, H., 2014. Identification of a CYP3A-like gene and CYPs mRNA expression modulation following exposure to benzo[a]pyrene in the bivalve mollusk *Chlamys farreri*. Mar. Environ. Res. 94, 7–15.

Toledo-Silva, Gd., Siebert, M.N., Medeiros, I.D., Sincero, T.C.M., Moraes, M.O., Goldstone, J.V., Bainy, A.C.D., 2008. Cloning a new cytochrome P450 isoform (CYP356A1) from oyster *Crassostrea gigas*. Mar. Environ. Res. 66, 15–18.

Wang, W.X., Meng, J., Weng, N., 2018. Trace metals in oysters: molecular and cellular mechanisms and ecotoxicological impacts. Environ. Sci. Process. Impacts 20, 892–912.

Werck-Reichhart, D., Feyereisen, R., 2000. Cytochromes P450: a success story. Genome Biol. 1. REVIEWS3003.

Wilcox, T.P., Zwickl, D.J., Heath, T.A., Hillis, D.M., 2002. Phylogenetic relationships of the dwarf boas and a comparison of Bayesian and bootstrap measures of phylogenetic support. Mol. Phylogenet. Evol. 25, 361–371.

Yue, Z., Zhang, X., Yu, Q., Liu, L., Zhou, X., 2018. Cytochrome P450-dependent reactive oxygen species (ROS) production contributes to Mn3O4 nanoparticle-caused liver injury. RSC Adv. 8, 37307–37314.

Zanette, J., Goldstone, J.V., Bainy, A.C., Stegeman, J.J., 2010. Identification of CYP genes in Mytilus (mussel) and Crassostrea (oyster) species: first approach to the full complement of cytochrome P450 genes in bivalves. Mar. Environ. Res. 69. Suppl, S1-3.

Zanette, J., Jenny, M.J., Goldstone, J.V., Parente, T., Woodin, B.R., Bainy, A.C., Stegeman, J.J., 2013. Identification and expression of multiple CYP1-like and CYP3-like genes in the bivalve mollusk Mytilus edulis. Aquat. Toxicol. 128-129, 101–112.

Zhang, C., Luo, X., Ni, X., Zhang, Y., Li, X., 2010. Functional characterization of cis-acting elements mediating flavone-inducible expression of CYP321A1. Insect Biochem. Mol. Biol. 40, 898–908.

Zhang, G., Fang, X., Guo, X., Li, L., Luo, R., Xu, F., Yang, P., Zhang, L., Wang, X., Qi, H., Xiong, Z., Que, H., Xie, Y., Holland, P.W., Paps, J., Zhu, Y., Wu, F., Chen, Y., Wang, J., Peng, C., Meng, J., Yang, L., Liu, J., Wen, B., Zhang, N., Huang, Z., Zhu, Q., Feng, Y., Mount, A., Hedgecock, D., Xu, Z., Liu, Y., Domazet-Loso, T., Du, Y., Sun, X., Zhang, S., Liu, B., Cheng, P., Jiang, X., Li, J., Fan, D., Wang, W., Fu, W., Wang, T., Wang, B., Zhang, J., Peng, Z., Li, Y., Li, N., Wang, J., Chen, M., He, Y., Tan, F., Song, X., Zheng, Q., Huang, R., Yang, H., Du, X., Chen, L., Yang, M., Gaffney, P.M., Wang, S., Luo, L., She, Z., Ming, Y., Huang, W., Zhang, S., Huang, B., Zhang, Y., Qu, T., Ni, P., Miao, G., Wang, J., Wang, Q., Steinberg, C.E., Wang, H., Li, N., Qian, L., Zhang, G., Li, Y., Yang, H., Liu, X., Wang, J., Yin, Y., Wang, J., 2012. The oyster genome reveals stress adaptation and complexity of shell formation. Nature 490, 49–54.

Zhang, J., Yao, J., Wang, R., Zhang, Y., Liu, S., Sun, L., Jiang, Y., Feng, J., Liu, N., Nelson, D., Waldbieser, G., Liu, Z., 2014. The cytochrome P450 genes of channel catfish: their involvement in disease defense responses as revealed by meta-analysis of RNA-Seq data sets. Biochim. Biophys. Acta 1840, 2813–2828.

Zhang, J.J., Li, H.J., Qin, Y.J., Ye, S., Liu, M., 2016. Identification of functional genes involved in Cd2+ response of Chinese surf clam (*Mactra chinensis*) through transcriptome sequencing. Environ. Toxicol. Pharm. 41, 113–120.

Zhang, X., Zong, C., Zhang, L., Garner, E., Sugie, S., Huang, C., Wu, W., Chang, J., Sakurai, T., Kato, M., Ichihara, S., Kumagai, S., Ichihara, G., 2018. Exposure of mice to 1,2-Dichloropropane induces CYP450-Dependent proliferation and apoptosis of Cholangiocytes. Toxicol. Sci. 162, 559–569.

Zhang, J., He, Y., Yan, X., Qu, C., Qi, P., 2019. Two novel CYP3A isoforms in marine mussel *Mytilus coruscus*: identification and response to cadmium and benzo[a] pyrene. Aquat. Toxicol. 214, 105239.